Biosensors and Bioelectronics ■ (■■■■) ■■■–■■■

Contents lists available at ScienceDirect

Biosensors and Bioelectronics

journal homepage: www.elsevier.com/locate/bios

A fluorescence resonance energy transfer (FRET) biosensor based on graphene quantum dots (GQDs) and gold nanoparticles (AuNPs) for the detection of mecA gene sequence of *Staphylococcus aureus*

Jingyu Shi [a], Chunyu Chan [a], Yukting Pang [a], Weiwei Ye [a], Feng Tian [a], Jing Lyu [a], Yu Zhang [b], Mo Yang [a,*]

[a] Interdisciplinary Division of Biomedical Engineering, The Hong Kong Polytechnic University, Hung Hom, Kowloon, Hong Kong, China
[b] Department of Mechanical Engineering, The Hong Kong Polytechnic University, Hung Hom, Kowloon, Hong Kong, China

ARTICLE INFO

Article history:
Received 6 June 2014
Received in revised form
22 September 2014
Accepted 22 September 2014

Keywords:
Graphene quantum dots (GQDs)
Gold nanoparticles (AuNPs)
Fluorescence resonance energy transfer (FRET)
Foodborne bacteria

ABSTRACT

In this work, a novel fluorescence resonance energy transfer (FRET) biosensor based on graphene quantum dots (GQDs) and gold nanoparticles (AuNPs) pairs was developed for *Staphylococcus aureus* specific gene sequence detection. This FRET biosensor platform was realized by immobilization of capture probes on GQDs and conjugation of reporter probes on AuNPs. Target oligos then co-hybridized with capture probes and reporter probes to form a sandwich structure which brought GQDs and AuNPs to close proximity to trigger FRET effect. The fluorescence signals before and after addition of targets were measured and the fluorescence quenching efficiency could reach around 87% with 100 nM target oligo. The limit of detection (LOD) of this FRET biosensor was around 1 nM for *S.aureus* gene detection. Experiments with both single-base mismatched oligos and double-base mismatched oligos demonstrated the good sequence selectivity of this FRET biosensor.

1. Introduction

Staphylococcus aureus (*S. aureus*) is a kind of notorious foodborne bacterium with the ability to produce heat-resistant toxins in food (Le Loir et al., 2003). *S. aureus* has become the second major bacteria in food poisoning, which threatens the health of both human and animals (Soriano et al., 2002). According to the USDA's economic research service, the infectious foodborne illness caused by *Staphylococcus* food poisoning is over 180 thousand cases annually in US (Leonard et al., 2003). Therefore, rapid and efficient detection of *S. aureus* is essential for providing the best treatment to the infected patients.

The conventional method for detecting *S. aureus* is primarily based on bacteria isolation, which is sensitive and inexpensive but bears the limitation of time-consuming and labor-intensive procedures (Carbonnelle et al., 2007; Xiao et al., 2007). Immunological assay such as enzyme-linked immunoabsorbent assay (ELISA) is a rapid method but suffers from relatively low sensitivity (Freed et al., 1982; Yazdankhah et al., 1998). Nucleic acid based assays such as polymerase chain reaction (PCR) have shown advantages of high sensitivity and high specificity for *S. aureus* detection (Carroll et al., 1996). However, the PCR method suffers from expensive equipment, complicated procedures and the need for skillful technicians.

Over the last decade, biosensing techniques have been used for rapid and sensitive foodborne bacteria detection (Alocilja and Radke, 2003; Yang et al., 2004; Yu et al., 2009; Chan et al., 2013). Among them, biosensors based on the hybridization between target DNA and capture DNA enables direct, sensitive, and rapid detection of bacterial DNA without target amplification (Pang et al., 2013). Various sensing mechanisms are developed for DNA detection such as quartz crystal microbalance (QCM) (Mao et al., 2006) and surface plasmon resonance (SPR) (Wang et al., 2011) and electrochemical biosensor (Wang et al., 2009; Luo et al., 2013). Fluorescence resonance energy transfer (FRET), which can transmit photo excitation energy from a donor fluorophore to an acceptor fluorophore, is a technique widely used in biosensing field (Storhoff et al., 2004; Gore et al., 2014). Traditional fluorophores include FAM, Texas red, and Cy5, which are limited by high cost and photobleaching effect. Therefore, they are not suitable for reliable and long term detection. In most recent years, graphene quantum dot (GQD) has received considerable attentions as fluorescence labels in biosensing due to its high brightness, long fluorescence lifetime, and good photo-stability (Zhang and Wang, 2012; Dong et al., 2012; Sun et al., 2013; Qian et al., 2014). GQD can be excited with a short-wavelength light source, usually in the UV

* Corresponding author. Fax: +852 2334 2429.
E-mail address: Mo.Yang@polyu.edu.hk (M. Yang).

http://dx.doi.org/10.1016/j.bios.2014.09.059
0956-5663/

region which is far away from acceptor emission spectrum and thus acceptor excitation can be minimized (Dong et al., 2012).

In this study, a novel FRET biosensor, with GQD and gold nanoparticle (AuNP) as the energy donor–acceptor pairs, is developed for *S. aureus* gene detection. AuNP is considered to be a kind of highly efficient fluorescence quencher due to its large surface area to volume ratio, easy surface functionalization, and strong surface plasma absorption in NIR-to-IR region (Anger et al., 2006; Zhu et al., 2010). Initially, capture probe and reporter probe was designed based on the sequence specific for *S. aureus mecA* gene and conjugated to GQDs and AuNPs respectively. FRET occurred when both capture probes and reporter probes were exposed to target oligos, allowing the hybridization between complimentary oligonucleotides pairs to bring GQDs to AuNPs into close proximity. Due to the fluorescence energy transfer from GQDs to AuNPs, the quenching of fluorescence intensity was recorded to quantify *S. aureus* target oligos. The detection of limit (LOD) of this GQDs–AuNPs FFET biosensor is around 1 nM for *S. aureus* gene sequence detection. Experiments with single-base-mismatched oligos and double-base-mismatched oligos were also explored and compared with complimentary target oligos to demonstrate the specificity of this FRET biosensor. As a result, this simple FRET biosensor has a low detection limit and good sequence selectivity.

2. Materials and methods

2.1. Materials

Gold (III) chloride trihydrate ($HAuCl_4 . 3H_2O$) and sodium citrate solution were purchased from Sigma Aldrich (St. Louis, MO, US). Graphene quantum dot (GQD) solution was purchased from Nanjing XFNANO Materials Tech Co., Ltd. (Jiangsu, Nanjing, China). 1-Ethyl-3-(3-dimethyl-aminopropyl) carbodiimide (EDC) was purchased from Sigma Aldrich. Oligonucleotides were synthesized and purified by Integrated DNA Technologies (IDT) Inc. (Coralville, IA, US). A 20-base gene sequence fragment of type II Staphylococcal cassette chromosome mecA gene (N315, GenBank: D86934.2) was used as the target (5′-ATTGGGATCATAGCGTCATT-3′). All of these chemicals were used as received without further purification. Thiol-modified capture probe oligonucleotide (A1): 5′-TGATCCCAAT/3ThioMC3-D/-3′, amine-modified reporter probe (G1): 5′-/5AmMC6/AATGACGCTA-3′, 20-mer complementary target probe (C1): 5′-ATTGGGATCATAGCGTCATT-3′, single-base-mismatched target probe (C2): 5′-ATTGGGAT**C**ATAGCGTCATT-3′, double-base-mismatched target to probe (C3): 5′-ATTGGGAT**C**ATAGC**G**TCATT-3′. All oligonucleotides were dissolved in distilled water to prepare stock solution. The bacteria genomic DNA sample was extracted from *S. aureus* strains (ATCC 29213) using an UltraCleanTM Microbial DNA Kit (MoBio Laboratories Inc., Carlsbad, CA). The PCR amplification targeting *mecA* gene was performed in a GeneAmp PCR System 9700 (Applied Biosystems, Foster, USA) with primers of Forward (5′-GATTACTTCAGAACCAGGTCAT-3′) and Reverse (5′-TAAACTGTGTCACACGATCCAT-3′).

2.2. Preparation of gold nanoparticles

Gold nanoparticles (AuNPs) with average size of 15 nm were prepared by the citrate reduction method (Ye et al., 2014). Briefly, a mixture of $HAuCl_4$ (3 μL, 14.3 wt%) and DI water (10 μL) were transferred to a clean beaker which was washed with aqua regia (mixture of HCl and HNO_3 at a 3:1 ratio) and then with DI water. Sodium citrate solution (1 mL, 1 wt%) was added to the boiling solution within one second upon vigorous stirring. The pale yellow solution turned wine red in a few minutes and was boiled for another 15 min. It then cooled down to room temperature by continuous stirring. The final product, AuNPs solution, was suspended in DI water and stored in refrigerator at 4 °C.

2.3. AuNPs–oligo conjugation

The thiol-modified probe oligo (A1: 5′-TGATCCCAA T/3ThioMC3-D/-3′, 64 μM) was treated with DTT (0.1 M, pH 8.2) for 40 min at room temperature to cleave disulfur linkage to enhance efficiency of subsequent oligo immobilization on AuNPs. The activated oligo was purified by gel-columns (illustra Microspin G-25 Columns, GE Healthcare, UK) with centrifugation at 3000 rpm for 2 min and characterized by a UV–visible spectrophotometer (Ultrospec 2100 pro). The purified oligos were mixed with a 500 μL AuNP solution prepared before. The mixture was then incubated at room temperature for 24 h. Then, sodium chloride solution (0.1 M NaCl, 5 mM $NaHPO_4$) was slowly added to allow for 16-h standing. The product was purified by centrifugation at 13,200 rpm for 30 min. The remaining red precipitate at the bottom was collected and rinsed 3 times with DI water to remove the unreacted reagents.

2.4. GQD–oligo conjugation

The purchased GQD solution (1 mg/mL) was firstly sonicated for 10 min. EDC (27 mM) solution was then added into the GQD suspensions. The mixture was shaken on a vortex mixer for 2 min and bath sonicated for another 15 min. After that, amine-modified capture probe (G1: 5′-/5AmMC6/AATGACGCTA-3′, 4.7 μM) was added into the mixture and incubated for 40 min at room temperature. The final product, GQD–oligo conjugate, was characterized by a spectrophotometer equipped with a 450 W steady-state xenon lamp (Edinburgh FLSP920).

2.5. FRET quenching

To investigate the effect of target oligo concentrations on fluorescence quenching efficiency, a fixed amount (1 mg/mL) of GQD-capture probe was incubated with different target oligo concentrations (100 pM to 400 nM) for 2 h to allow hybridization at room temperature. A 50 μL solution of the above mixture was then mixed with a 50 μL reporter probe modified AuNP solution for incubation of 2 h at room temperature to form a co-hybridized sandwich complex structure. After incubation, the fluorescence intensity was measured using a Tecan Infinite F200 micro-plate reader. All the fluorescence intensity was recorded under the same condition. The specificity of the system was also evaluated with both single mismatched oligos and double-base mismatched oligos.

2.6. Characterization

The morphology and size of GQDs and AuNPs were characterized using a JEOL-2100F transmission electron microscopy (TEM) equipped with an Oxford Instrument EDS system, operating at 200 kV. Samples for TEM were prepared on holey carbon coated 400 mesh copper grids. A UV–visible spectrophotometer (Ultrospec 2100 pro) was used for AuNPs adsorption spectra measurement. A FLS920P Edinburgh analytical spectrophotometer was used for GQD emission spectra measurement.

Please cite this article as: Shi, J., et al., Biosensors and Bioelectronics (2014), http://dx.doi.org/10.1016/j.bios.2014.09.059

3. Results

3.1. Mechanism of FRET biosensor

The sensing mechanism of the proposed GQD–AuNP FRET biosensor for *S. aureus* gene detection is shown in Fig. 1. Here, GQDs and AuNPs acted as donor and acceptor of FRET pairs, respectively. Initially, amine modified capture probes (a) were immobilized on the GQDs surface while AuNPs were conjugated with reporter probes (b). The added target *S. aureus* gene oligo (a′b′) co-hybridized with capture probes (a) on GQDs and reporter probes (b) on AuNPs, which brought GQDs and AuNPs into close proximity. Under 365 nm light excitation, the emission of GQDs was absorbed by AuNPs. By measuring the fluorescence intensity change of the solution, *S. aureus* target oligos can be detected.

3.2. Characterization of GQDs and AuNPs

The AuNPs were synthesized by the citrate reduction method. TEM experiment was performed to characterize the morphology and size of AuNPs. As shown in Fig. 2a, the synthesized AuNPs had good round shape and uniform size with the average diameter of 15 nm. Fig. 2b shows the well-dispersed GQDs with the average size of 3 ± 1 nm. Fig. 2c shows a TEM image after conjugation of AuNPs with GQDs. It was observed that the large AuNPs were surrounded by many small GQDs to form a satellite structure through oligo hybridization. Zeta potential measurement was used to characterize the conjugation between oligos and AuNPs/GQDs. As shown in Fig. S1, the initial zeta potential values of AuNPs, GQDs and oligos at pH=7 are −39.5 mV, −15.2 mV and −26.6 mV, respectively. After conjugation, oligo probes cover the whole surface of AuNPs and GQDs and the zeta potential of AuNP–oligo and GQD–oligo become −26.5 mV and −25.5 mV at pH=7 respectively, which are close to the zeta potential of pure oligos. The zeta potential measurement results demonstrated the successful conjugation of oligos to AuNPs and GQDs. FTIR spectra were also used for conjugation characterization. Fig. S2 shows the FTIR spectra of GQDs and GQD–oligo. For GQD–oligo FTIR spectrum, the characteristic absorption peaks appear at 1655 cm^{-1} and 1585 cm^{-1} indicating the presence of amide vibration, which confirms the successfully formation of the amide bond between GQDs and amine modified oligos via the EDC/NHS method. The feature band of oligos at 1116 cm^{-1} stands for the vibration of symmetric phosphate (PO_2–). Additionally, absorption peak at 1060 cm^{-1} is typically assigned to the C–O stretch of DNA backbone and absorption band at 965 cm^{-1} is an indication of P–O stretching. Fig. S3 shows the FTIR spectra of AuNPs and AuNPs–oligo. AuNPs show the presence of both carboxyl groups (–COOH, 1600 cm^{-1}) and hydroxyl functional groups (−OH, 3400 cm^{-1}). After oligo conjugation, AuNPs–oligo shows characteristic

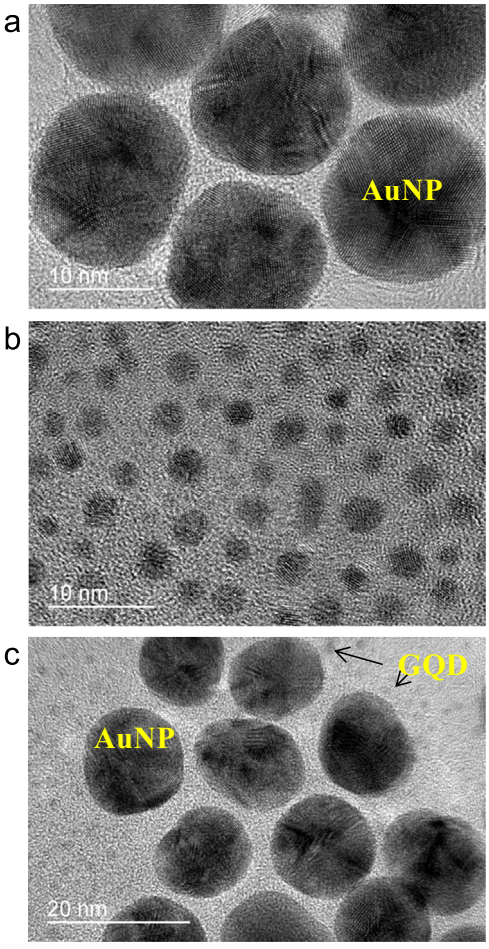

Fig. 2. TEM images of (a) synthesized AuNPs with average size of 15 nm; (b) GQDs with average size of 3 nm; (c) AuNPs conjugated with GQDs.

vibration bands from 1250 cm^{-1} to 850 cm^{-1} assigned to the phosphate groups of oligos and small peaks around 2900 cm^{-1} indicating the –CH_2– stretching, which confirm the conjugation of oligos onto AuNPs.

3.3. Emission spectra of GQDs–oligo and absorption spectra of AuNPs–oligo

The optical emission properties of GQDs vary with the density of sp^2 sites and GQDs size which can be used to tune the energy gap of GQDs (Eda et al., 2010; Loh et al., 2010). Under 365 nm excitation, GQDs emit intense blue light with the emission band around 460 nm (inset of Fig. 3a). Real samples are usually comprised of complex mixtures which may lead to false results

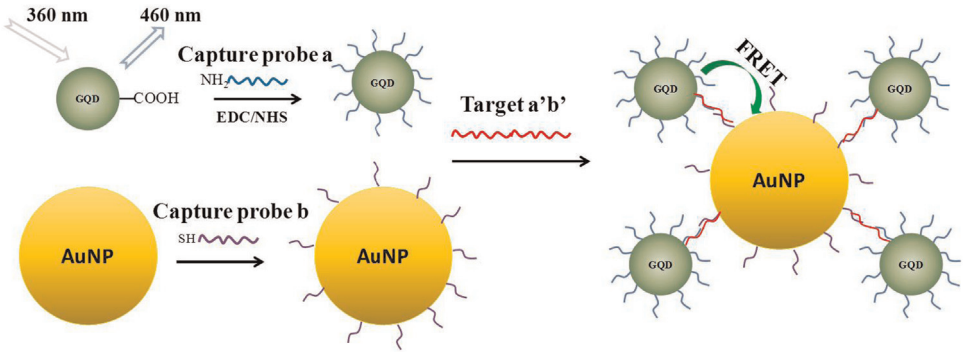

Fig. 1. The sensing mechanism of the proposed GQDs–AuNPs FRET biosensor for *S. aureus* gene detection.

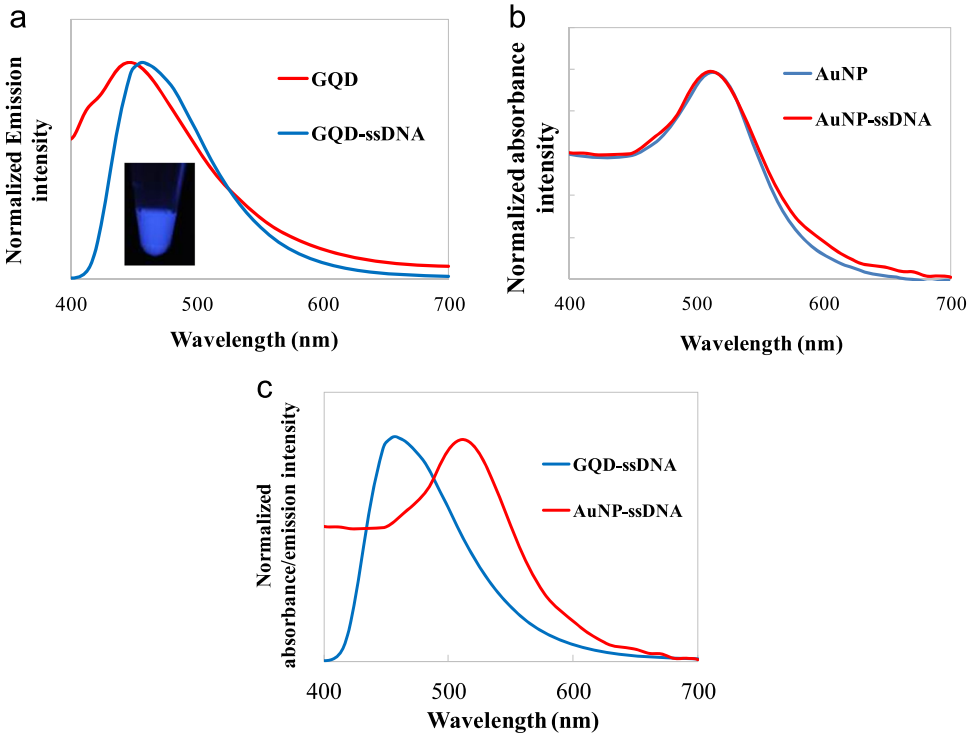

Fig. 3. (a) Emission spectra of GQDs before and after conjugation with oligos; (b) absorption spectra of AuNPs before and after conjugation with oligos; (c) spectra overlapping between emission spectra of GQDs and absorption spectra of AuNPs. (For interpretation of the references to color in this figure, the reader is referred to the web version of this article.)

or poor precision. It is necessary to consider the potential interferences caused by matrix effects. For GQD FRET biosensor of this experiment, the main matrix effect will be pH value and H^+ ion strength in the solution. Generally, GQDs show a pH dependent photo luminescence (PL) emission property. In acidic solution, PL intensities of GQDs decrease dramatically because of the interaction between free zigzag sites of the GQDs and H^+ ions, which hampers the emissive state in PL (Peng et al., 2012). In alkaline solution, PL intensities of GQDs also decrease and accompany with blue shift of emission peaks (Zhu et al., 2012). Therefore, in order to get strong blue fluorescence emission, the best working pH range should be from 6 to 8, which is neutral pH value. In this experiment, we used neutral buffer solution with pH=7.4 to achieve the strong blue fluorescence emission.

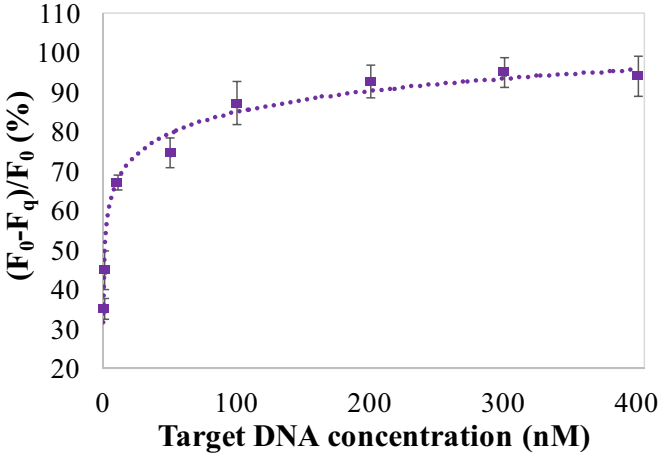

Fig. 4. The quenching efficiency $Q=1-F_q/F_0$ versus with a series of target oligo concentrations.

GQDs dispersed well in water solution due to the abundant oxygen-containing functional groups on the surface, which was demonstrated by the uniform blue color distribution in GQD solution. After conjugation with oligos, the peak of emission spectra of GQDs slightly shifted to the right (Fig. 3a). The adsorption spectra of AuNPs also slightly shifted to the right after conjugation with oligos with the main adsorption region in the range of 450–550 nm (Fig. 3b). The spectra overlapping between emission spectra of GQDs and absorption spectra of AuNPs ensured the feasibility of this FRET biosensor (Fig. 3c).

3.4. Construction of FRET biosensor for target gene detection

To explore the quenching efficiency of this FRET biosensor, a series of concentrations of target oligos were tested from 100 pM to 400 nM. Herein, a fixed amount of 1 mg/mL GQD conjugated with capture probes was used. As a result of sandwich assay structure formation of GQDs–oligo–AuNPs, GQDs were brought close to AuNPs surface and fluorescence quenching was realized. The quenching efficiency is expressed by $Q=1-F_q/F_0$, where F_q is the fluorescence intensity of GQDs after quenching, and F_0 is the original fluorescence intensity of GQDs. As shown in Fig. 4, the quenching efficiency gradually increased with the increase of concentrations of target oligos and reached a value of 87% with 100 nM target oligos. The quenching efficiency almost unchanged when the concentration of target oligos further increased. Fig. 5 shows the fluorescence signal quenching (F_0-F_q) versus a series of target oligos concentrations. Then quenching effect decreased with the decrease of target oligos. The limit of detection (LOD) is determined by the control signal plus three times of noise signal (standard derivation), which was around 1 nM.

The PCR amplified product of *S. aureus mecA* gene was further detected by this FRET biosensor under the same conditions with synthesized target oligo. Regular PCR was performed using the template DNA extracted from *S. aureus* strains with the

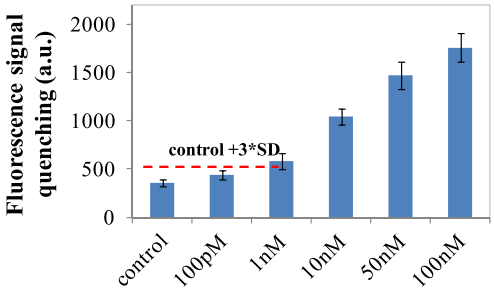

Fig. 5. The fluorescence signal quenching (F_0-F_q) versus a series of target oligo concentrations from 100 pM to 100 nM.

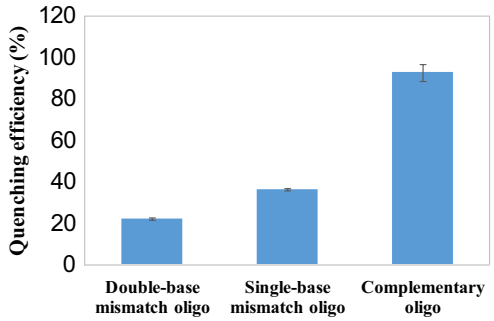

Fig. 6. Quenching efficiency comparison among single-base mismatched oligos, double-base mismatched oligos, and complimentary target oligo with concentration of 200 nM.

concentration of 1.0×10^2 CFU/mL, which gave a final gene size of 287 bp. Fig. S4 shows the emission spectra of this FRET biosensor after hybridization with the PCR product (corresponding to *S. aureus* concentration of 1.0×10^2 CFU/mL). An obvious fluorescence signal reduction was observed after hybridization with the PCR product of *mecA* gene, which was much larger than that of PCR solution without genomic DNA template. This experiment demonstrated the possibility of adaption of this FRET biosensor for real biological sample detection.

3.5. Specificity of FRET biosensor

To explore the specificity of this GQDs–AuNPs FRET biosensor, both single-base mismatched oligos and double-base mismatched oligos were used to compare with the complementary target oligos. All the experiments used the same concentration of 200 nM for comparison. As shown in Fig. 6, the quenching efficiency decreased significantly with the increasing number of mismatches. The quenching efficiency for complementary target oligo was around 93%, while that of single-base mismatched oligos and double-base mismatched oligos dropped to 37% and 22% respectively. Generally, an increasing number of mismatches of target oligos would lead to decreasing duplex stability, which decreased the chances to form GQDs–oligos–AuNPs sandwich complex and QGDs emission would not decrease much. Similar results have also been reported (Yang et al., 2008; Tao et al., 2012; Li et al., 2011). The results indicated that this FRET biosensor exhibits high selectivity.

The current methods for *S. aureus* DNA detection include polymerase chain reaction (PCR) (Brakstad et al., 1992; Alarcon et al., 2006), surface plasmon resonance (SPR) (Nawattanapaiboon et al., 2014), and fluorescence microarray (Wilson et al., 2002; Bally et al., 2006). Although PCR has high sensitivity and good specificity for *S. aureus* DNA detection with limit of detection (LOD) in the pM scale, it suffers from complex sample preparation steps (Brakstad et al., 1992). SPR has high sensitivity with LOD from around tens of pM to 1 nM for *S. aureus* DNA detection. However, SPR is very sensitive to non-specific adsorption on surface which leads to the poor specificity (Nawattanapaiboon et al., 2014). As an optical detection method, fluorescence microarray has advantages of easy operation, direct readout and good specificity but have relatively low sensitivity with LOD from tens of nM to μM due to the low fluorescence brightness and short fluorescence lifetime (Wilson et al., 2002; Bally et al., 2006). As a proof of concept, our GQD based FRET biosensor achieves a LOD of 1 nM which has better sensitivity than that of fluorescence microarray and comparable to that of SPR biosensor. Moreover, our GQD biosensor has good specificity due to the sandwich assay structure. The FRET effect is only triggered when target fully match both reporter probes on GQDs and AuNPs.

4. Conclusion

In this paper, a novel FRET biosensor based on GQDs and AuNPs pairs was developed for *S. aureus* specific gene detection. The sandwich structure formation caused by co-hybridization of target oligos with capture probes and reporter probes brought GQDs and AuNPs into close proximity to trigger FRET phenomena. The quenching efficiency was measured with a series of target gene oligos concentrations and the results demonstrated the feasibility of this FRET biosensor for bacteria gene detection with LOD of 1 nM. The experiments with single-base mismatched oligos and double-base mismatched oligos demonstrated the good sequence selectivity of this FRET biosensor. In this study, a short gene sequence of the whole genome of *S. aureus* was used as target oligos. In real applications, the targets should be the whole genome of bacteria extracted from raw samples. This GQDs–AuNPs FRET biosensor will be adapted for the whole genome of *S. aureus* detection in the future, which has the potential to be used as a simple, sensitive and portable platform for in-field foodborne pathogen detection in food safety and environmental screening.

Acknowledgement

This work was supported by the Hong Kong Research Council General Research Grant (PolyU5305/11E) and the Hong Kong Ph. D Fellowship Scheme Fund (HKPF10-13386/ PolyU RUY5).

Appendix A. Supplementary information

Supplementary data associated with this article can be found in the online version at http://dx.doi.org/10.1016/j.bios.2014.09.059.

References

Alocilja, E.C., Radke, S.M., 2003. Biosens. Bioelectron. 18, 841–846.
Alarcon, B., Vicedo, B., Aznar, R., 2006. J. Appl. Microbiol. 100, 352–364.
Anger, P., Bharadwaj, P., Novotny, L., 2006. Phys. Rev. Lett. 96, 113002.
Bally, M., Halter, M., Voros, J., Grandin, H.M., 2006. Surf. Interface Anal. 38, 1442–1458.
Brakstad, O.G., Aasbakk, K., Maeland, J.A., 1992. J. Clin. Microbiol. 30, 1654–1660.
Carbonnelle, E., Beretti, J.L., Cottyn, S., Quesne, G., Berche, P., Nassif, X., Ferroni, A., 2007. J. Clin. Microbiol. 45, 2156–2161.
Carroll, K.C., Leonard, R.B., Newcomb-Gayman, P.L., Hillyard, D.R., 1996. Am. J. Clin. Pathol. 106, 600–605.
Chan, K.Y., Ye, W.W., Zhang, Y., Xiao, L.D., Leung, P.H.M., Li, Y., Yang, M., 2013. Biosens. Bioelectron. 41, 532–537.
Dong, Y., Shao, J., Chen, C., Li, H., Wang, R., Chi, Y., Lin, X., Chen, G., 2012. Carbon 50, 4738–4743.
Eda, G., Lin, Y.Y., Mattevi, C., Yamaguchi, H., Chen, H.A., Chen, I.S., Chen, C.W., Chhowalla, M., 2010. Adv. Mater. 22, 505–509.

Freed, R.C., Evenson, M.L., Reiser, R.F., Bergdoll, M.S., 1982. Appl. Environ. Microbiol. 44, 1349–1355.
Gore, A.H., Kale, M.B., Anbhule, P.V., Patil, S.R., Kolekar, G.B., 2014. RSC Adv. 4, 683–692.
Le Loir, Y., Baron, F., Gautier, M., 2003. Genet. Mol. Res. 2, 63–76.
Leonard, P., Hearty, S., Brennan, J., Dunne, L., Quinn, J., Chakraborty, T., O'Kennedy, R., 2003. Enzym. Microb. Technol. 32, 3–13.
Li, H.L., Zhang, Y.W., Luo, Y.L., Sun, X.P., 2011. Small 7, 1562–1568.
Luo, C., Tang, H., Cheng, W., Yan, L., Zhang, D., Ju, H., Ding, S., 2013. Biosens. Bioelectron. 48, 132–137.
Loh, K.P., Bao, Q.L., Eda, G., Chhowalla, M., 2010. Nat. Chem. 2, 1015–1024.
Mao, X., Yang, L., Su, X.L., Li, Y., 2006. Biosens. Bioelectron. 21, 1178–1185.
Nawattanapaiboon, K., Kiatpathomchai, W., Santanirund, P., Wongsakulyanon, A., Sutapun, B., Srikhirin, T., 2014. IFMBE Proc. 43, 845–848.
Pang, S., Gao, Y., Li, Y., Liu, S., Su, X., 2013. Analyst 138, 2749–2754.
Peng, J., Gao, W., Gupta, B.K., Liu, Z., Romero-Aburto, R., Ge, L.H., Song, L., Alemany, L.B., Zhan, X.B., Gao, G.H., 2012. Nano Letters 12, 844–849.
Qian, Z.S., Shan, X.Y., Chai, L.J., Ma, J.J., Chen, J.R., Feng, H., 2014. Nanoscale 6, 5671–5674.
Soriano, J.M., Font, G., Moltó, J.C., Mañes, J., 2002. Trends Food Sci. Technol. 13, 60–67.
Storhoff, J.J., Marla, S.S., Bao, P., Hagenow, S., Mehta, H., Lucas, A., Viswanadham, G., Müller, U.R., 2004. Biosens. Bioelectron. 19, 875–883.
Sun, H., Wu, L., Wei, W., Qu, X., 2013. Mater. Today 16, 433–442.
Tao, Y., Lin, Y.H., Huang, Z.Z., Ren, J.S., Qua, X.G., 2012. Analyst 137, 2588–2592.
Wang, J., Luo, Y., Zhang, B., Chen, M., Huang, J., Zhang, K., Gao, W., Fu, W., Jiang, T., Liao, P., 2011. J. Transl. Med. 9, 1–9.
Wang, L.J., Liu, Q.J., Hu, Z.Y., Zhang, Y.F., Wu, C.S., Yang, M., Wang, P., 2009. Talanta 78, 647–652.
Wilson, W.J., Strout, C.L., DeSantis, T.Z., Stilwell, J.L., Carrano, A.V., Andersen, G.L., 2002. Mol. Cell. Probes 16, 119–127.
Xiao, X., Yang, X., Liu, T., Chen, Z., Chen, L., Li, H., Deng, L., 2007. Appl. Microbiol. Biotechnol. 75, 1209–1216.
Yang, L.J., Li, C.L., Griffis, C.L., Johnson, M.G., 2004. Biosens. Bioelectron. 19, 1139–1147.
Yang, R.H., Jin, Y.Y., Chen, Y., Shao, N., Kang, H.Z., Xiao, Z.Y., Tang, Z.W., Wu, Y.R., Zhu, Z., Tan, W.H., 2008. J. Am. Chem. Soc. 130, 8351–8358.
Yazdankhah, S.P., Hellemann, A.L., Rønningen, K., Olsen, E., 1998. Vet. Microbiol. 62, 17–26.
Ye, W.W., Shi, J.Y., Chan, C.Y., Zhang, Y., Yang, M., 2014. Sens. Actuators B: Chem. 193, 877–882.
Yu, J.J., Liu, Z.B., Liu, Q.J., Yuen, K.T., Mak, A.F.T., Yang, M., Leung, P.H.M., 2009. Sens. Actuators A—Phys. 154, 288–294.
Zhang, Y., Wang, T.H., 2012. Theranostics 2, 631–654.
Zhu, J., Li, J.J., Wang, A.Q., Chen, Y., Zhao, J.W., 2010. Nanosc. Res. Lett. 5, 1496–1501.
Zhu, S.J., Zhang, J.H., Liu, X., Li, B., Wang, X.F., Tang, S.J., Meng, Q.N., Li, Y.F., Shi, C., Hu, R., Yang, B., 2012. RSC Adv. 7, 2717–2720.

Please cite this article as: Shi, J., et al., Biosensors and Bioelectronics (2014), http://dx.doi.org/10.1016/j.bios.2014.09.059